

PART FOUR  
THEORY OF WIRELESS PROPAGATION  
OF UHF RADIO WAVES  
IN COAL MINE TUNNELS

PART FOUR  
THEORY OF WIRELESS PROPAGATION  
OF UHF RADIO WAVES  
IN COAL MINE TUNNELS

TABLE OF CONTENTS

	<u>Page</u>
List of Tables	4.iv
List of Figures	4.v
INTRODUCTION	4.1
I. RAY THEORY	4.3
II. WAVE METHOD	4.4
III. COMPARISON WITH EXPERIMENT	4.6
IV. DIFFUSE RADIATION CALCULATIONS	4.10
A. ROUGHNESS EFFECTS	4.11
B. TILT EFFECTS	4.12
C. COUPLING OF INDIVIDUAL MODES	4.14
V. PROPAGATION AROUND A CORNER	4.16
VI. EFFECT OF ANTENNA ORIENTATION	4.23
VII. INSERTION LOSS	4.24
VIII. OVERALL LOSS IN A STRAIGHT TUNNEL	4.26
IX. OVERALL LOSS ALONG A PATH WITH ONE CORNER	4.29
X. CONCLUSIONS	4.33
XI. REFERENCES	4.34
APPENDIX A - RAY METHOD	4.35
APPENDIX B - WAVE METHOD	4.37
APPENDIX C - COUPLING OF $E_h$ and $E_v$ MODES	4.43

PART FOUR  
THEORY OF WIRELESS PROPAGATION  
OF UHF RADIO WAVES  
IN COAL MINE TUNNELS

TABLE OF CONTENTS  
(Continued)

	<u>Page</u>
APPENDIX D - PROPAGATION AROUND A CORNER	4.49
APPENDIX E - ANTENNA INSERTION LOSS BY CURRENT- DISTRIBUTION METHOD	4.53
APPENDIX F - EXPECTED COMMUNICATION RANGE BETWEEN TWO ROVING MINERS	4.55

PART FOUR  
THEORY OF WIRELESS PROPAGATION  
OF UHF RADIO WAVES  
IN COAL MINE TUNNELS

LIST OF TABLES

<u>Table No.</u>	<u>Title</u>	<u>Page</u>
I	Diffuse Radiation Component in Main Tunnel and at Beginning of Cross Tunnel	4.18
II	Excitation of $E_h$ Mode in Cross Tunnel by Diffuse Component in Main Tunnel	4.20
III	Effect of Antenna Orientation	4.24
IV	Insertion Loss ( $L_i$ ) (For a Half-Wave Antenna)	4.26
V	Calculation of Overall Loss for $E_h$ Mode with Two Half Wave Dipole Antennas	4.27
VI	Overall Loss Along a Path Including One Corner $E_h$ Mode with Half Wave Dipole Antennas	4.32
A1	Ray Method Calculations (For $E_h$ Mode)	4.36
B1	Loss Rates for Various Modes	4.42
C1	Coupling Between $E_h$ and $E_v$ Modes	4.48

PART FOUR  
THEORY OF WIRELESS PROPAGATION  
OF UHF RADIO WAVES  
IN COAL MINE TUNNELS

LIST OF FIGURES

<u>Figure No.</u>	<u>Title</u>	<u>Page</u>
1	Refraction Loss for $E_h$ and $E_v$ Modes in High Coal	4.7
2	Refraction Loss for $E_h$ Mode in Low Coal	4.8
3	Resultant Propagation Loss for $E_h$ Mode in High Coal (Refraction, Wall Roughness and Tilt)	4.15
4	Corner Loss in High Coal - 415 MHz	4.21
5	Corner Loss in High Coal - 1000 MHz	4.22
6	Total Loss for Various Distances Along a Straight Tunnel	4.28
7	Overall Loss in a Straight Tunnel in High Coal (for Isotropic Antennas) - 415 MHz	4.30
8	Overall Loss in a Straight Tunnel in High Coal (for Isotropic Antennas) - 1000 MHz	4.31
C1	Incident and Reflected Fields Relative to a Rotated Portion of the Roof of the Tunnel	4.44
D1	Geometry for Coupling to Cross Tunnels	4.50
F1	Predicted UHF Wireless Radio Coverage	4.56

PART FOUR

THEORY OF WIRELESS PROPAGATION  
OF UHF RADIO WAVES  
IN COAL MINE TUNNELS

INTRODUCTION

This Part is concerned with the theoretical study of UHF radio communication in coal mines, with particular reference to the rate of loss of signal strength along a tunnel, and from one tunnel to another around a corner. Of prime interest are the nature of the propagation mechanism and the prediction of the radio frequency which propagates with the smallest loss. Our theoretical results are compared with measurements made by Collins Radio Co.

This work was conducted as part of the Pittsburgh Mining and Safety Research Center's investigation of new ways to reach and extend two-way communications to the key individuals that are highly mobile within the sections and haulage ways of coal mines.

At frequencies in the range of 200-4,000 MHz the rock and coal bounding a coal mine tunnel act as relatively low loss dielectrics with dielectric constants in the range 5-10. Under these conditions a reasonable hypothesis is that transmission takes the form of waveguide propagation in a tunnel, since the wavelengths of the UHF waves are smaller than the tunnel dimensions. An electromagnetic wave traveling along a rectangular tunnel in a lossless dielectric medium can propagate in any one of a number of allowed waveguide modes. All of these modes are "lossy modes" owing to the fact that any part of the wave that impinges on a wall of the tunnel is partially refracted into the surrounding dielectric and partially reflected back into the waveguide. The refracted part propagates away from the waveguide and represents a power loss. This type of waveguide mode differs from the light-pipe modes in glass fibers in which total internal reflection occurs at the wall of the fiber, with zero power loss if the fiber and the matrix in which it is embedded are both lossless. It is to be noted that the attenuation rates of the waveguide modes studied in this paper depend almost entirely on refraction loss, both for the dominant mode and higher modes excited by scattering, rather than on ohmic loss. The effect of ohmic loss due to the small conductivity of the surrounding material is found to be negligible at the frequencies of interest here, and will not be further discussed.

The study reported here is concerned with tunnels of rectangular cross-section and the theory includes the case where the dielectric constant of the material on the side walls of the tunnel is different from that on top and bottom walls. The work extends the earlier theoretical work by Marcatili and Schmeltzer<sup>(1)</sup> and by Glaser<sup>(2)</sup> which applies to waveguides of circular and parallel-plate geometry in a medium of uniform dielectric constant.

## I. RAY THEORY

The allowed modes in a rectangular tunnel in a dielectric can be determined approximately either by a ray theory or a wave theory approach. In the ray method we consider a ray of the radiation which bounces from wall to wall of the tunnel making a grazing angle  $\phi_1$  with the side walls and  $\phi_2$  with the floor and roof. The propagation modes with the lowest attenuation rates are the two (1, 1) modes which have the electric field, E, polarized predominantly in the horizontal and vertical directions, respectively. These two modes, which we will refer to as the  $E_h$  and  $E_v$  modes, are both defined in the ray picture by the phase relations

$$\sin\phi_1 = \frac{\lambda}{2d_1} \quad (1)*$$

$$\sin\phi_2 = \frac{\lambda}{2d_2} \quad (2)$$

where  $\lambda$  is the free space wavelength of the radiation and  $d_1$ ,  $d_2$  are the horizontal and vertical dimensions of the tunnel. Equations (1) and (2) are the conditions that the phase shift undergone by the ray is exactly  $360^\circ$  after successive reflections from the two side walls or from the floor and roof.

For frequencies around 1,000 MHz,  $\lambda$  is small compared with  $d_1$  and  $d_2$ . Therefore we can use the approximate relations

$$\phi_1 = \frac{\lambda}{2d_1} \quad (3)$$

$$\phi_2 = \frac{\lambda}{2d_2} \quad (4)$$

The numbers of reflections  $N_1$  and  $N_2$  experienced by a ray at the vertical and horizontal walls of the tunnel, while traveling a distance  $z$  along the tunnel, are given by

$$N_1 = \frac{z\phi_1}{d_1} \quad (5)$$

$$N_2 = \frac{z\phi_2}{d_2} \quad (6)$$

The attenuation factor for the ray intensity for this distance is

$$\frac{I}{I_0} = R_1^{N_1} R_2^{N_2} \quad (7)$$

where  $R_1$  and  $R_2$  are the power reflectances of the vertical and horizontal surfaces at the grazing angles  $\phi_1$  and  $\phi_2$ , respectively.

---

\* References to Figures, Tables and Equations apply to those in this Part unless otherwise noted.

On combining equations (3)-(7) we find for the loss L in decibels

$$L = 5\lambda z \left( \frac{1}{d_1^2} \log_{10} \frac{1}{R_1} + \frac{1}{d_2^2} \log_{10} \frac{1}{R_2} \right) \quad (8)$$

In using this formula to calculate the loss rate one must calculate  $R_1$  and  $R_2$  by means of the standard Fresnel reflection formulas for the angles  $\phi_1$  and  $\phi_2$ , and the corresponding dielectric constants  $K_1$  and  $K_2$ . The result is different for the  $E_h$  and  $E_v$  modes because the Fresnel formulas are different for the two polarizations. Appendix A gives the Fresnel formulas and ray-method calculations for the  $E_h$  mode.

## II. WAVE METHOD

In the wave method we obtain an approximate solution of Maxwell's equations for lossy modes in a rectangular waveguide with dielectric walls. We use Cartesian coordinates with origin at the center of the tunnel cross-section, the z-axis along the tunnel axis, the x-axis horizontal, and the y-axis vertical. In the case of the  $E_h$  mode the main field components of the mode are given approximately by

$$E_x = E_o \cos k_1 x \cos k_2 y e^{-ik_3 z} \quad (9)$$

$$H_y = \frac{k_3}{\omega\mu_o} E_o \cos k_1 x \cos k_2 y e^{-ik_3 z} \quad (10)$$

where the symbols have their customary meaning and

$$k_1^2 + k_2^2 + k_3^2 = k_o^2 = 4\pi^2/\lambda^2. \quad (11)$$

In addition to these transverse field components there are small longitudinal components  $E_z$  and  $H_z$  and a small transverse component  $H_x$ .

The simple solution given by (9) and (10), along with the small longitudinal and transverse components, does not allow the boundary conditions of continuity of the tangential components of E and H to be accurately satisfied over the whole surface of the waveguide. An approximation to the boundary conditions gives values for  $k_1$  and  $k_2$  as follows:

$$k_1 \cong \frac{\pi}{d_1} \left( 1 - \frac{2iK_1}{k_0 d_1 \sqrt{K_1 - 1}} \right) \quad (12)$$

$$k_2 \cong \frac{\pi}{d_2} \left( 1 - \frac{2i}{k_0 d_2 \sqrt{K_2 - 1}} \right) \quad (13)$$

where  $K_1$  and  $K_2$  are the dielectric constants of the sidewalls and of the floor and roof, respectively.

From (11)-(13) we obtain the imaginary part of the wave number z-component  $k_3$  and from it the power loss over a distance z. The result in decibels is

$$L_{Eh} = 4.343\lambda^2 z \left( \frac{K_1}{d_1^3 \sqrt{K_1 - 1}} + \frac{1}{d_2^3 \sqrt{K_2 - 1}} \right) . \quad (14)$$

In like manner the loss for the  $E_v$  mode is found to be

$$L_{Ev} = 4.343\lambda^2 z \left( \frac{1}{d_1^3 \sqrt{K_1 - 1}} + \frac{K_2}{d_2^3 \sqrt{K_2 - 1}} \right) . \quad (15)$$

These results show that the loss rate increases with the square of the wavelength and decreases with the cube of the linear dimensions of the tunnel. Losses calculated by (14) and (15) agree closely with those calculated by the ray loss formula (8). Since (14) and (15) do not require evaluation of the Fresnel reflectances  $R_1$  and  $R_2$ , they are considerably simpler to use. Details of the wave theory, including loss calculations for higher modes, are given in Appendix B.

### III. COMPARISON WITH EXPERIMENT

Figure 1 shows loss rates in dB/100 ft. as functions of frequency calculated by equations (14) and (15) for the  $E_h$  and  $E_v$  modes in a tunnel of width 14 ft. and height, 7 ft., representative of a haulage way in a seam of high coal, for  $K_1 = K_2 = 10$ , corresponding to coal on all the walls of the tunnel. It is seen that the loss rate is much greater for the  $E_v$  mode. Figure 2 shows the calculated  $E_h$  loss rate for a tunnel of half the height. The higher loss rate is due to the effect of the  $d_2^3$  term in equation (14).

Two experimental values obtained by Collins Radio Co.<sup>(3)</sup> for horizontal-horizontal antenna orientations are also shown in Figure 1. These values agree well with theory for the  $E_h$  mode for 415 MHz, but not so well at 1,000 MHz. The departure suggests that some additional loss mechanism sets in at higher frequencies.

It is also to be noted that the experimental values of the loss rates for all three orientation arrangements of the transmitting and receiving dipole antennas, namely, horizontal-horizontal, vertical-horizontal, and vertical-vertical, are surprisingly close to each other. The independence of loss rate with respect to polarization is not predicted by the theory discussed so far, as seen in Figure 1 for the  $E_h$  and  $E_v$  modes. Indeed the theory predicts no transmission at all for the VH antenna arrangement.

FIGURE 1  
 REFRACTION LOSS FOR  $E_h$  AND  $E_v$  MODES  
 IN HIGH COAL

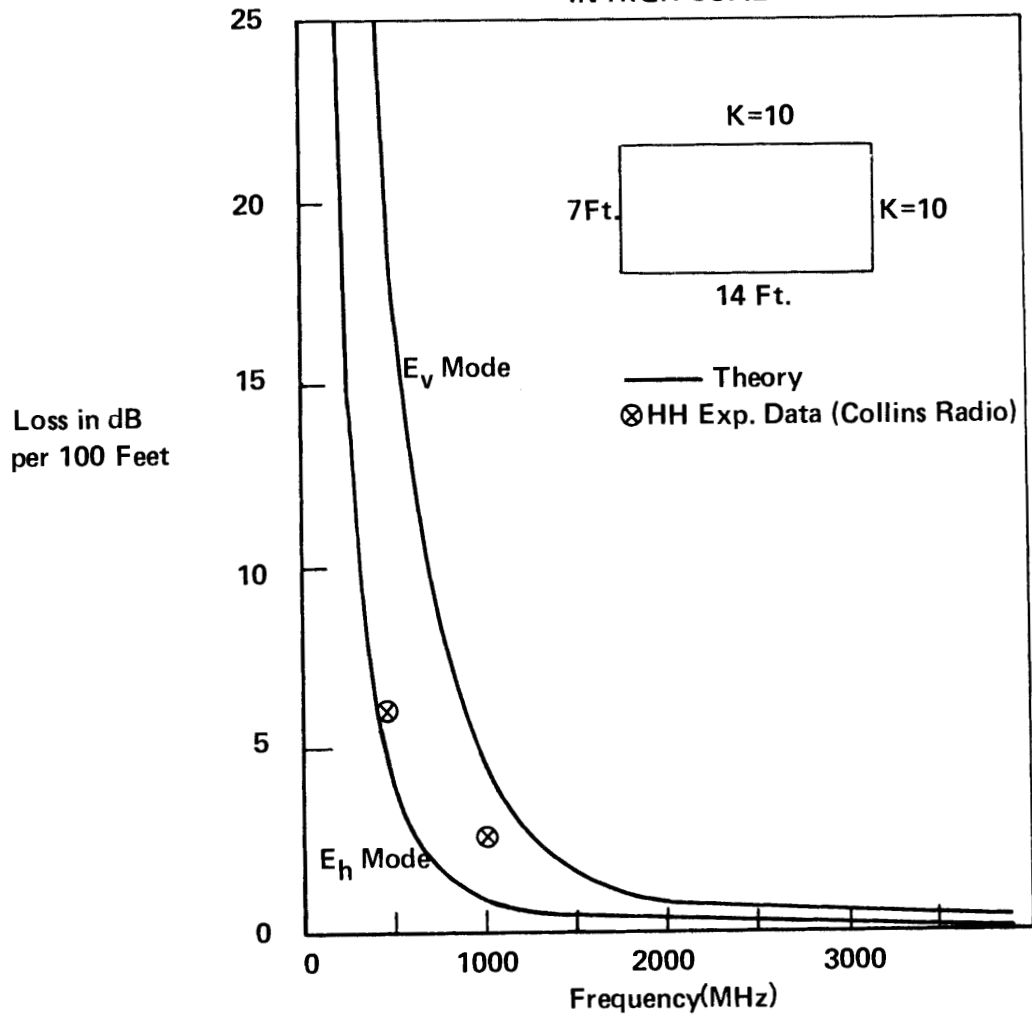
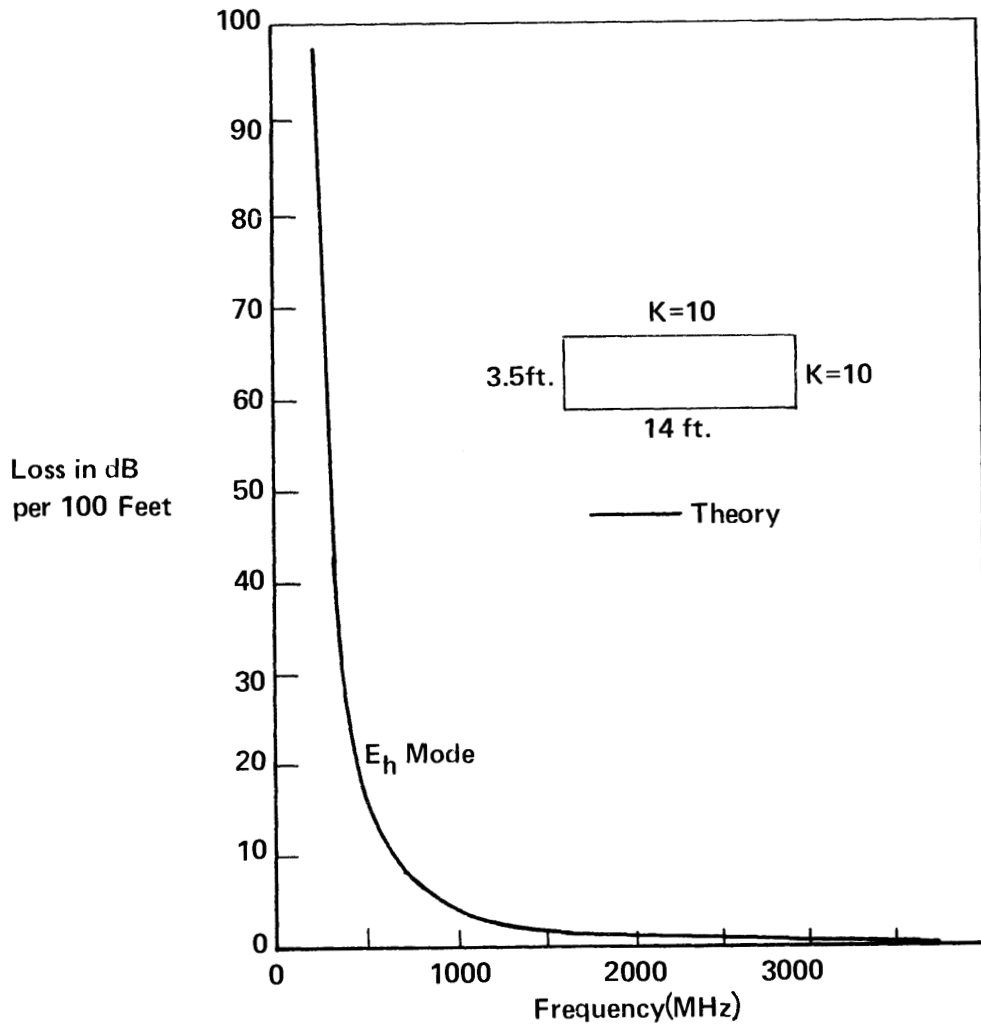


FIGURE 2  
REFRACTION LOSS FOR  $E_h$  MODE IN LOW COAL



To explain both the higher observed loss rate at the higher frequencies, relative to the calculated  $E_h$  mode values, and the independence of the loss rate on antenna orientation, we postulate that roughness and variable tilt of the four tunnel walls combine to cause scattering of the dominant  $E_h$  mode. The scattered radiation goes into many higher modes and can be regarded as a diffuse component that accompanies the  $E_h$  mode. The diffuse component is in dynamical equilibrium with the  $E_h$  mode in the sense that its rate of generation by the  $E_h$  mode is balanced by its rate of loss by refraction into the surrounding dielectric. Since the diffuse component consists of higher waveguide modes for which the refractive loss rate is much higher than for the fundamental  $E_h$  mode, the dynamical balance point is such that the level of the diffuse component is many dB below that of the  $E_h$  mode at any point in the tunnel.

The scattering loss from the  $E_h$  mode into the diffuse component begins to increase rapidly when the wavelength is so short that the mode grazing angles  $\phi_1$  and  $\phi_2$ , defined earlier, become comparable with the root mean square tilt of the walls of the tunnel. This accounts for the higher experimental loss at 1,000 MHz than that predicted for the  $E_h$  mode by the theory for a perfect dielectric waveguide shown in Figure 1.

The diffuse radiation component also accounts for the observed independence of loss rate on antenna orientation. The argument here is that, irrespective of whether the transmitting antenna is oriented horizontally or vertically, at a sufficient distance down the tunnel the radiation ultimately settles down into the dominant  $E_h$  component and a weaker diffuse component. If the transmitting antenna is oriented vertically it initially excites the  $E_v$  mode which dies out relatively rapidly by refractive loss and scattering into the unpolarized diffuse component. The diffuse component in turn couples to the  $E_h$  mode which, owing to its much lower loss rate finally becomes dominant. When dynamical

equilibrium is reached the diffuse component remains at a fixed number of dB below the  $E_h$  mode. Therefore a vertically oriented receiving antenna carried down the tunnel measures the loss rate of the  $E_h$  mode. A horizontal receiving antenna measures the  $E_h$  mode directly and the loss rate is the same as before although the insertion loss of the antenna is considerably less.

Experiments by Collins Radio Co. on the signal strength transmitted around a corner into a cross tunnel give further convincing proof of the diffuse component hypothesis. They found that a large loss occurred when the receiving antenna was moved around the corner, but that the received signal strength was then independent of antenna orientation. This is exactly what one would expect from the diffuse radiation hypothesis since the well collimated  $E_h$  mode in the main tunnel couples very weakly into the cross tunnel, whereas the uncollimated diffuse component couples fairly efficiently. Since the diffuse radiation is likely to be largely unpolarized the observed independence of signal strength on antenna orientation is understandable.

Another observation by Collins Radio is that the initial attenuation rate on entering the cross tunnel is much higher than the rate in the main tunnel. This is also in accord with the diffuse radiation component which has a much larger loss rate than the  $E_h$  mode owing to its steeper angles of incidence on the tunnel walls.

#### IV. DIFFUSE RADIATION CALCULATIONS

We discuss two different mechanisms by which diffuse radiation is generated by scattering out of the dominant  $E_h$  mode. The first of these is roughness of the walls of the tunnel which is here regarded as variations in local surface level relative to the mean surface level. The second is long range tilt of the tunnel walls relative to the mean planes which define the dimensions  $d_1$  and  $d_2$  of the tunnel.

### A. Roughness Effects

When a parallel beam of radiation of intensity  $I_0$  strikes a rough surface at normal incidence the reflected radiation consists of a parallel beam of reduced intensity  $I$  together with a diffuse component. If the surface is a perfect reflector

$$I = I_0 e^{-2\left(\frac{2\pi h}{\lambda}\right)^2} \quad (16)$$

where  $\lambda$  is the wavelength and  $h$  is the root mean square roughness. For incidence at a grazing angle  $\phi$  one may assume that the effective roughness is now  $h \sin\phi$ , so the loss factor becomes<sup>(4)</sup>

$$f = e^{-2\left(\frac{2\pi h \sin\phi}{\lambda}\right)^2} \quad (17)$$

In the case of the dominant mode in a dielectric waveguide we can from equations (1) and (2) write for the roughness loss factors per reflection for the vertical and horizontal walls:

$$f_1 = e^{-2\left(\frac{\pi h}{d_1}\right)^2} \quad (18)$$

$$f_2 = e^{-2\left(\frac{\pi h}{d_2}\right)^2} \quad (19)$$

The loss factor for a distance  $z$  is therefore, from equations (3)-(6)

$$f = e^{-2N_1\left(\frac{\pi h}{d_1}\right)^2 - 2N_2\left(\frac{\pi h}{d_2}\right)^2} \approx e^{-\pi^2 h^2 \lambda \left(\frac{1}{d_1^4} + \frac{1}{d_2^4}\right) z} \quad (20)$$

The loss in dB is then

$$L_{\text{roughness}} = 4.343\pi^2 h^2 \lambda \left( \frac{1}{d_1} + \frac{1}{d_2} \right) z \quad (21)$$

### B. Tilt Effects

The effect of wall tilt can be estimated as follows. Suppose that a ray of the  $E_h$  mode encounters a portion of a side wall that is tilted through a small angle  $\theta$  about a vertical axis. Then the reflected beam is rotated through an angle  $2\theta$ . This means that the electric field is changed from

$$E_x = F(x,y) e^{-ik_3 z} \quad (22)$$

to

$$E_x' = F(x,y) e^{-ik_3 (z \cos 2\theta + x \sin 2\theta)} \quad (23)$$

The power coupling factor  $g_1$  of the disturbed field (23) back into the mode (22) is given by

$$g_1 = \frac{|\iint E_x \bar{E}_x' dx dy|^2}{\iint |E_x|^2 dx dy \iint |E_x'|^2 dx dy} \quad (24)$$

where the integrations are over the cross-section of the tunnel. The bar over  $E_x$  indicates complex conjugate. Since  $\theta$  is small we can replace  $\cos 2\theta$  by 1 and  $\sin 2\theta$  by  $2\theta$ . Then (24) becomes

$$g_1 = \frac{|\iint |F|^2 e^{2ik_3 x \theta} dx dy|^2}{(\iint |F|^2 dx dy)^2} \quad (25)$$

Instead of using the actual function  $\cos k_1 x \cos k_2 y$  for  $F$ , we find it more convenient to use an equivalent Gaussian function

$$F = F_0 e^{-\left(\frac{x^2}{a^2} + \frac{y^2}{b^2}\right)} \quad (26)$$

and integrate over infinite limits. The result is

$$g_1 = e^{-\frac{1}{2} k_3^2 a^2 \theta^2} \quad (27)$$

Next we assume that  $F^2$  falls to  $1/e$  at the point  $x = d_1/2$ ,  $y = 0$ , which is at the surface of the waveguide. Then  $a^2 = 1/2 d_1^2$  and

$$g_1 = e^{-\frac{1}{4} k_3^2 d_1^2 \theta^2} \quad (28)$$

Likewise, tilting of the floor or roof gives a coupling factor

$$g_2 = e^{-\frac{1}{4} k_3^2 d_2^2 \theta^2} \quad (29)$$

The loss factor for a distance  $z$  is

$$g = g_1^{N_1} g_2^{N_2} = e^{-\frac{\pi^2 \theta^2 z}{\lambda}} \quad (30)$$

where we have replaced  $k_3$  by  $k_0$ .

The loss in dB is therefore

$$L_{\text{Tilt}} = \frac{4.343 \pi^2 \theta^2 z}{\lambda} \quad (31)$$

On comparing equation (21) with equation (31) we see that whereas the roughness loss depends strongly on the waveguide dimensions the tilt loss is independent of them. Another important difference is that the roughness increases with wavelength while the tilt loss decreases.

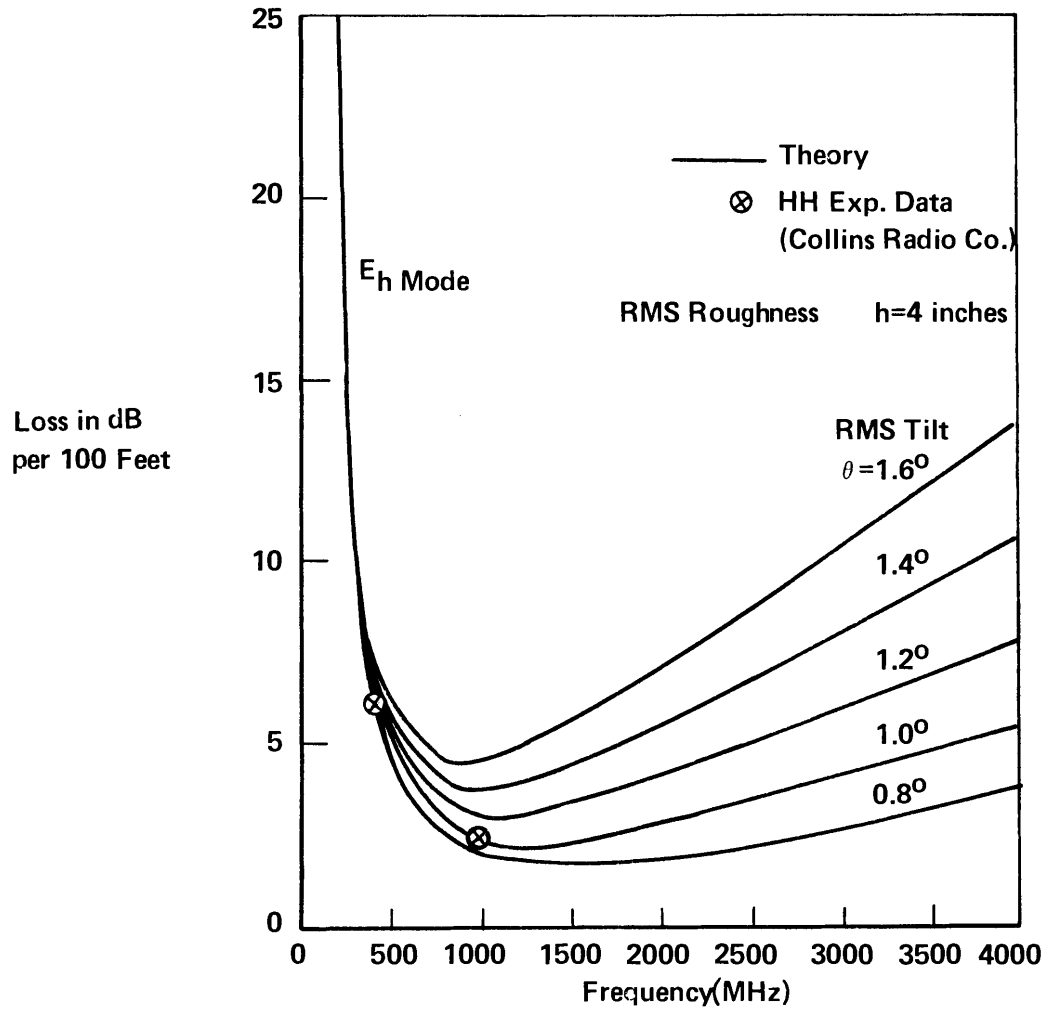
Figure 3 shows the effect on the  $E_h$  mode propagation of adding the loss rates due to roughness and tilt to the refraction loss given in Figure 1. The curves are calculated for a root mean square roughness of 4 inches and for various assumed values of the root mean square tilt angle  $\theta$ . It is seen that a value  $\theta = 1^\circ$  gives good agreement with the experimental values measured by Collins Radio Co. The effect of tilt is much greater than that of roughness.

The results indicate that for a 14 ft. x 7 ft. tunnel in a medium of dielectric constant 10 the optimum frequency is about 1,000 MHz.

### C. Coupling of Individual Modes

The diffuse radiation method is a convenient first approximation to the solution of the difficult problem of the mutual interactions of all the allowed waveguide modes caused by irregularities of the waveguide walls. As a first step in this interaction problem we have considered the coupling between the (1,1)  $E_h$  and  $E_v$  modes due to longitudinal ridges on the roof of the tunnel. The results of the calculation are given in Appendix C.

FIGURE 3  
 RESULTANT PROPAGATION LOSS FOR  $E_h$  MODE IN HIGH COAL  
 (Refraction, Wall Roughness and Tilt)



## V. PROPAGATION AROUND A CORNER

As mentioned earlier, signal propagation from a main tunnel around a corner into a cross tunnel arises from the diffuse component that accompanies the  $E_h$  mode wave in the main tunnel. The intensity  $I_d$  of this diffuse component in the main tunnel relative to the intensity  $I_h$  of the  $E_h$  mode is given by the relation

$$\frac{I_{d,\text{main}}}{I_{h,\text{main}}} = \frac{L_{hd}}{L_d} \quad (32)$$

where  $L_{hd}$  is the loss rate from the  $E_h$  mode into the diffuse component and  $L_d$  is the loss rate of the diffuse component by refraction.

To calculate  $L_d$  approximately, we take the loss rate to be that of an "average" ray of the diffuse component having direction cosines  $(1/\sqrt{3}, 1/\sqrt{3}, 1/\sqrt{3})$ . Then

$$L_d = 10 \left( \frac{z}{d_1} + \frac{z}{d_2} \right) \log_{10} \frac{1}{R} \quad (33)$$

where  $R$  is the Fresnel reflectance of the average ray at the walls of the tunnel.  $R$  is 0.28 for the case  $K_1 = K_2 = 10$ . Then for  $d_1 = 14$  ft.,  $d_2 = 7$  ft.,  $z = 100$  ft., we find that  $L_d = 119$  dB/100 ft. This value has to be corrected for the loss of diffuse radiation into cross tunnels which we assume have the same dimensions as the main tunnel and occur every 75 ft. From relative area considerations we find that this loss is 2 dB/100 ft. The corrected value is therefore

$$L_d = 121 \text{ dB/100 ft} \quad (34)$$

which is independent of frequency.

The loss rate  $L_{hd}$  is shown in Table I as a function of frequency for the 14 ft. x 7 ft. tunnel. The values are the sum of the roughness and tilt losses calculated by equations (21) and (31) for a roughness of 4 inch rms and tilt of  $1^\circ$  rms. The ratio  $I_{d,\text{main}} / I_{h,\text{main}}$ , calculated by equation (32) and expressed in dB, is also shown. It is seen that the diffuse component is larger at the higher frequencies. The reason is that scattering out of the  $E_h$  mode due to tilt increases with frequency.

From solid angle considerations (see Appendix D) one finds that the fraction of diffuse radiation in the main tunnel that enters the 14 ft. x 7 ft. aperture of the cross tunnel is 0.15 or -8.2 dB. The diffuse level just inside the aperture of the cross tunnel, relative to the  $E_h$  wave in the main tunnel is shown in the last column of Table I, which is obtained by subtracting 8.2 dB from the numbers in column 4. A dipole antenna placed at this point and oriented either horizontally or vertically responds to half of the diffuse component or 3 dB less than the figures in column 5. At 1,000 MHz, for example, the signal received by an antenna at this point is -30.2 dB relative to that received in the main tunnel with the antenna oriented horizontally. At 415 MHz the corresponding number is -31.8 dB. These values agree moderately well with the measurements of Collins Radio Co.

The diffuse radiation that enters the cross tunnel decays at a rate of 121 dB/100 ft., according to the rather crude "average" ray approximation. This means that at 100 ft. down the cross tunnel the signal level at 1,000 MHz should be -151 dB. However, the level measured by Collins Radio is about -68dB. We attribute this large difference to the fact that the diffuse component in the main tunnel excites the  $E_h$  mode in the cross tunnel, and that this mode travels down the cross tunnel with much less attenuation than the diffuse component.

To calculate the coupling of the diffuse component in the main tunnel into the  $E_h$  mode in the cross tunnel, we determine the fraction

TABLE I  
 DIFFUSE RADIATION COMPONENT IN MAIN TUNNEL  
 AND AT BEGINNING OF CROSS TUNNEL

f (MHz)	$\lambda$ (Ft.)	$L_{hd}$ (dB/100 ft.)	$\frac{I_{d, main}}{I_{h, main}}$ (dB)	$\frac{I_{d, cross}}{I_{h, main}}$ (dB)
4,000	.245	5.4	-13.5	- 21.7
3,000	.327	4.1	-14.7	- 22.9
2,000	.49	2.8	-16.4	- 24.6
1,000	.98	1.5	-19.0	- 27.2
415	2.37	1.1	-20.6	- 28.8
200	4.92	1.3	-19.7	- 27.9

$(I_{h, \text{cross}})/(I_{d, \text{main}})$  of diffuse radiation leaving the exit aperture of the main tunnel which lies within the solid angle of acceptance of the  $E_h$  mode in the cross tunnel. The result (see Appendix D) is

$$\frac{I_{h, \text{cross}}}{I_{d, \text{main}}} = \frac{\lambda^3}{16\pi d_1^2 d_2} \quad (35)$$

This ratio is given in dB in Table II.

The  $E_h$  level in the cross tunnel relative to the  $E_h$  level in the main tunnel is found by adding column 2 in Table II and column 4 in Table I. The result is shown as  $(I_{h, \text{cross}}/I_{h, \text{main}})_0$  in Table II. At 100 ft. down the cross tunnel we find the corresponding ratio by adding the loss rate given in Figure 3 for a tilt of  $1^\circ$ . The result is shown in the last column of Table II. The value of -70.1 dB at 1,000 MHz agrees very well with the measured value of -68 dB.

Our model of the propagation around a corner into a cross tunnel therefore consists of a relatively strong diffuse component at the beginning of the cross tunnel at a level of around -20 to -30 dB together with a much weaker  $E_h$  mode at a level of -50 to -80 dB, depending on frequency. These two components propagate down the cross tunnel with a very high loss rate of around 120 db/100 ft. for the diffuse component, and a very low loss rate for the  $E_h$  component. Therefore the  $E_h$  component overtakes the diffuse component at about 100 ft. down the tunnel, while the radiation changes its character from almost completely unpolarized to very highly polarized. This description of the propagation is in good general agreement with measurement, as shown in Figures 4 and 5.

TABLE II

EXCITATION OF  $E_h$  MODE IN CROSS TUNNEL  
 BY DIFFUSE COMPONENT IN MAIN TUNNEL

f (MHz)	$\frac{I_{h, \text{cross}}}{I_{d, \text{main}}}$ (dB)	$\left(\frac{I_{h, \text{cross}}}{I_{h, \text{main}}}\right)_0$ (dB)	$\left(\frac{I_{h, \text{cross}}}{I_{h, \text{main}}}\right)_{100'}$ (dB)
4,000	-66.7	-80.2	85.6
3,000	-62.9	-77.6	81.8
2,000	-57.7	-74.1	77.1
1,000	-48.6	-67.6	70.1
415	-37.1	-57.7	64.1
200	-27.6	-47.3	71.6

FIGURE 4  
CORNER LOSS IN HIGH COAL

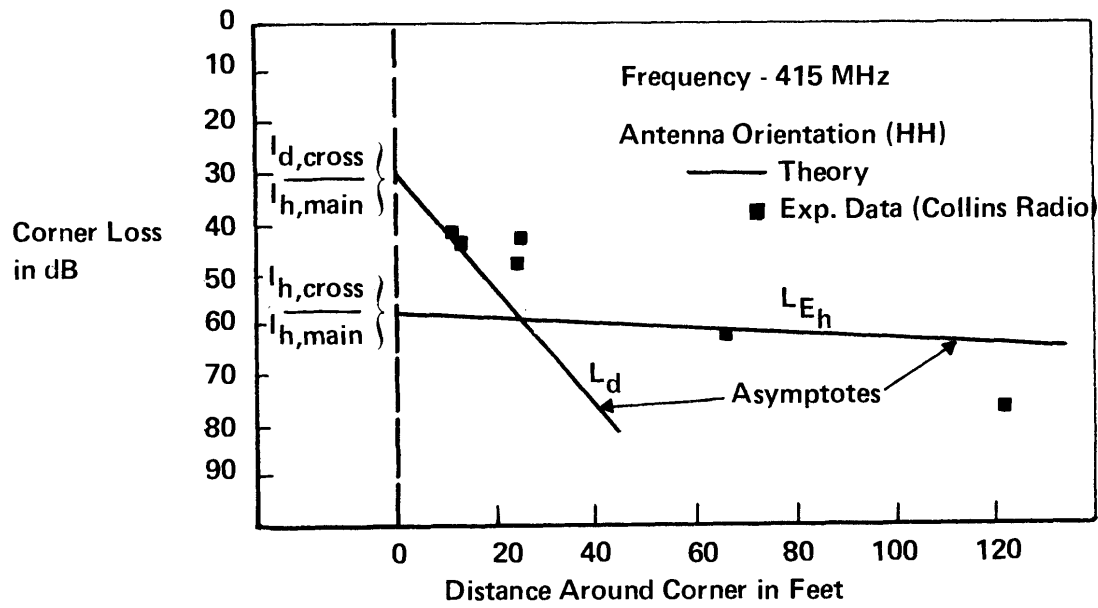
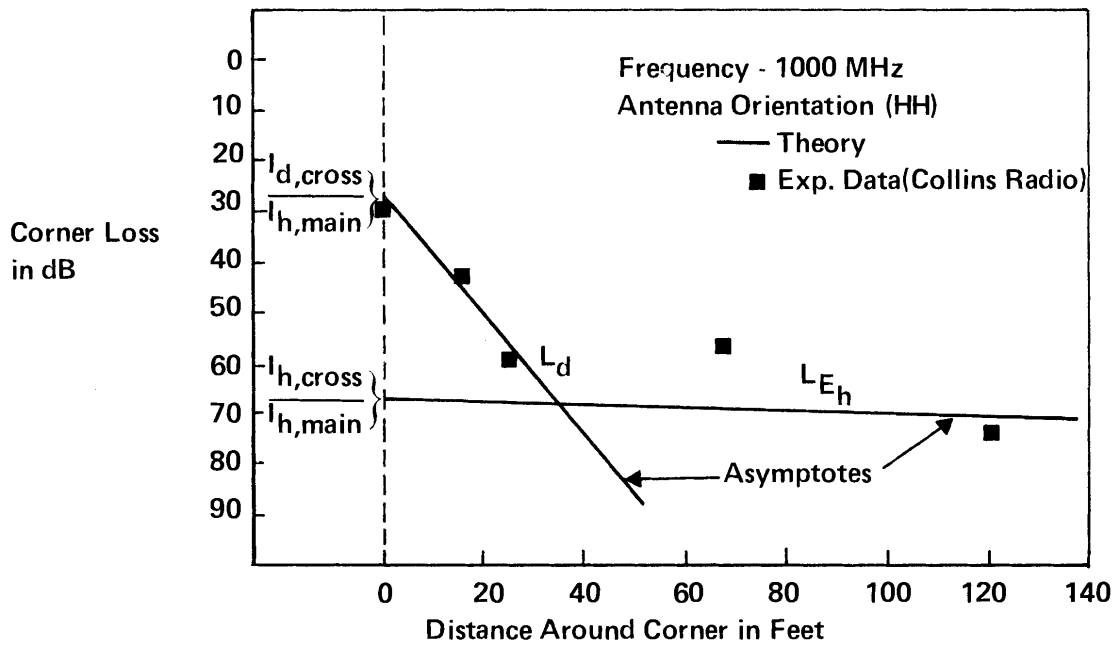


FIGURE 5  
CORNER LOSS IN HIGH COAL



## VI. EFFECT OF ANTENNA ORIENTATION

We now return to the effect on signal loss of the orientations of the transmitting and receiving antennas. In the case of identical antennas the principle of reciprocity states that the VH and HV losses are equal, where the first and second letters signify the orientation of the transmitting and receiving antennas, respectively. We will assume that the actual antennas are so small compared with the dimensions of the tunnel that interactions with the tunnel are negligible and therefore reciprocity is still valid.

We also invoke the principle that at great distances down the tunnel the radiation consists of the  $E_h$  mode together with a related diffuse component, for either orientation of the transmitting antenna.

From these two principles it follows that the HV or VH loss in dB is half way between HH and VV losses, or that

$$VV - HH = 2(HV-HH) \quad (36)$$

Now we obtain the relative loss HV-HH by subtracting 3 dB from column 4 of Table I. The results are shown in Table III along with VV-HH calculated from (36). The last column in the Table gives average experimental values of VV-HH determined by Collins Radio Co. Since no data were obtained by Collins for a horizontal transmitting antenna at 200 MHz, we have doubled their reported value of -25 dB for VV-VH at this frequency.

Comparison of theory and experiment in Table III indicates that the average value of VV-HH is predicted quite well by the theory but the variation with frequency is not well predicted. The discrepancy may result from failure of the reciprocity principle owing to the fact that a  $\lambda/4$  groundplane transmitting antenna was used whereas the receiving

TABLE III  
EFFECT OF ANTENNA ORIENTATION

f (MHz)	HH (dB)	HV (dB)	VH (dB)	VV (dB)
1000	0	-22.0	-22.0	-44.0
415	0	-23.6	-23.6	-47.2
200	0	-22.7	-22.7	-45.4

antenna was a standard dipole antenna of the type normally used for field strength measurements. However, the data for 415 MHz agree well with the theory since VH appears to be about halfway between HH and VV over a considerable distance down the tunnel.

#### VII. INSERTION LOSS

Dipole or whip antennas are the most convenient for portable radio communications between individuals. However, a considerable loss of signal power occurs at both the transmitter and receiver when simple dipole antennas are used, because of the inefficient coupling of these antennas to the waveguide mode. The insertion loss of each antenna can be calculated by two methods.

In the first method we make use of the effective transmitting or receiving area  $A_{ant}$  of a half-wave dipole antenna which is given by

$$A_{ant} = \frac{1.64\lambda^2}{4\pi} \quad (37)$$

The coupling factor  $C$  to the  $E_h$  waveguide mode is then, from (9),

$$C = \frac{|\int_{A_{ant}} E_o \cos k_1 x \cos k_2 y dA|^2}{\int_{A_{guide}} |E_o \cos k_1 x \cos k_2 y|^2 \int_{A_{ant}} dA} \quad (38)$$

where  $A_{\text{guide}}$  is the area of cross-section of the waveguide. At frequencies on the order of 1,000 MHz where the wavelengths become small compared to tunnel cross-section dimensions, the cosine factors of the (1,1)  $E_h$  mode are approximately zero at the walls of the tunnel and  $A_{\text{ant}} \ll A_{\text{guide}}$ . Under these conditions (38) gives approximately

$$C \cong \frac{4A_{\text{ant}}}{A_{\text{guide}}} \cos^2\left(\frac{\pi x_0}{d_1}\right) \cos^2\left(\frac{\pi y_0}{d_2}\right) \quad (39)$$

for a dipole centered at  $x_0, y_0$  in the tunnel. When the dipole is placed at the center of the tunnel (39) reduces to

$$C \cong \frac{4A_{\text{ant}}}{A_{\text{guide}}} = \frac{1.64}{\pi} \frac{\lambda^2}{d_1 d_2} \quad (40)$$

In the second method we make use of a standard microwave circuit technique for computing the amount of power coupled into a waveguide mode by a probe. A half-wave dipole antenna centered at  $x_0, y_0$  in the tunnel and oriented in the x-direction is approximated by a surface current distribution, and the power coupled into the (1,1)  $E_h$  mode by the current distribution is compared with the power radiated by the dipole in free space. The coupling coefficient so obtained is shown in Appendix E to be

$$C = 0.52 \frac{\lambda^2}{d_1 d_2} \cos^2\left(\frac{\pi x_0}{d_1}\right) \cos^2\left(\frac{\pi y_0}{d_2}\right) \quad (41)$$

which is numerically equal to (39), and therefore to (40), when the dipole is located at the center of the tunnel ( $x_0 = y_0 = 0$ ).

The insertion loss  $L_i$  is then

$$L_i = -10 \log_{10} \left(0.52 \frac{\lambda^2}{d_1 d_2}\right) \quad (42)$$

for a dipole centrally located in the tunnel. Table IV gives values of  $L_i$  for various frequencies, for a 14 ft. x 7 ft. tunnel.

TABLE IV  
 INSERTION LOSS ( $L_i$ )  
 (For a Half-Wave Antenna)

F (MHz)	$\lambda$ (Feet)	$L_i$ (dB)
4000	0.245	35.0
3000	0.327	32.4
2000	0.49	28.9
1000	0.98	22.9
415	2.37	15.2
200	4.92	8.9

It is seen that the insertion loss decreases rapidly with increasing wavelength, as one would expect, since the antenna size occupies a larger fraction of the width of the waveguide. The overall insertion loss, for both antennas, is twice the value given in the Table. A considerable reduction in the loss would result if high gain antenna systems were used.

#### VIII. OVERALL LOSS IN A STRAIGHT TUNNEL

The overall loss in signal strength in a straight tunnel is the sum of the propagation loss and the insertion losses of the transmitting and receiving antennas. Table V lists the component loss rates for the  $E_h$  mode due to direct refraction, roughness, and tilt; the total propagation loss rate; the insertion loss for two half-wave antennas; and the overall loss for three different distances. The results are also shown in Figure 6, where it is seen that the optimum frequency for minimum overall loss is the range 500-1000 MHz, depending on the desired communication distance.\*

It is also of interest to combine the results in Table V with those in Table IV to obtain the overall loss versus distance for the HH, HV (or VH), and VV antenna orientation. In order to compare the theoretical

---

\* For roving miner mobile applications using portable transceivers, some frequency independent factors accounting for polarization, efficiency and fade margin losses, should also be applied to these results, as described in Appendix F, to obtain practical estimates of communication range.

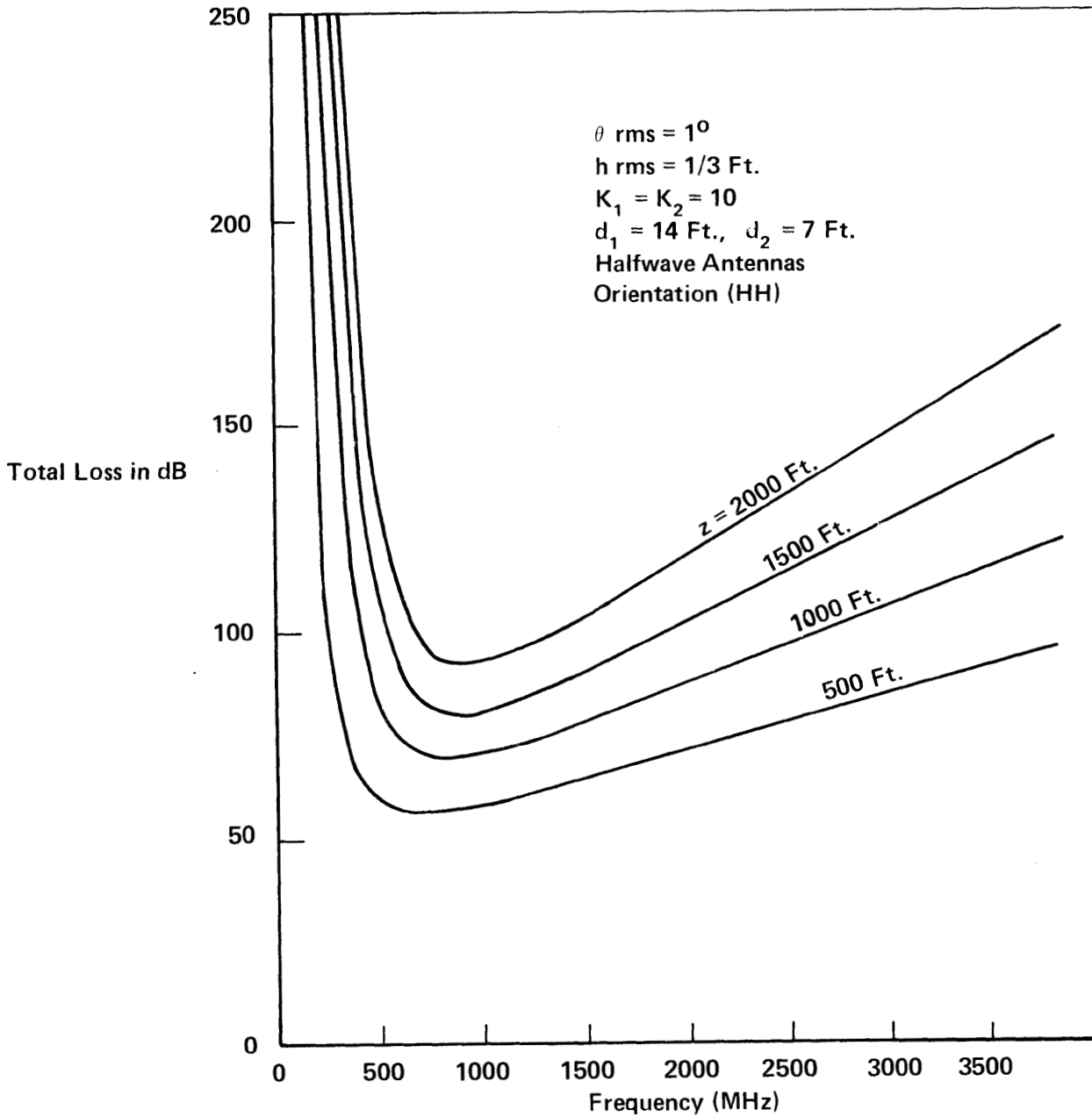
TABLE V  
 CALCULATION OF OVERALL LOSS FOR E<sub>h</sub> MODE WITH TWO HALFWAVE DIPOLE ANTENNAS

(h = 1/3 Ft.  $\theta = 1^\circ$ ,  $K_1 = K_2 = 10$ ,  $d_1 = 14$  Ft.,  $d_2 = 7$  Ft.)

f (MHz)	L <sub>refraction</sub> (dB/100')	L <sub>roughness</sub> (dB/100')	L <sub>tilt</sub> (dB/100')	L <sub>propagation</sub> (dB/100')	L <sub>insertion</sub> (dB)	L <sub>overall</sub> (dB)				
						100'	500'	1000'	1500'	2000'
4000	.06	.05	5.33	5.44	69.90	75	97	124	152	179
3000	.10	.07	3.99	4.16	64.88	69	86	107	127	148
2000	.23	.10	2.66	2.99	57.86	61	73	88	103	118
1000	.91	.21	1.33	2.45	45.82	48	58	70	81	93
415	5.34	.50	0.55	6.39	30.48	37	62	94	126	158
200	23.00	1.04	0.27	24.31	17.80	42	139	261	383	504
100	92.00	2.08	0.14	94.20	5.80	100	477	948	1419	1890

FIGURE 6

TOTAL LOSS FOR VARIOUS DISTANCES ALONG A STRAIGHT TUNNEL



values with the experimental data of Collins Radio Co., which are expressed with reference to isotropic antennas, we add 4.3 dB to the overall loss calculated for half-wave dipoles. The theoretical results for the three different antenna orientations for frequencies of 415 MHz and 1,000 MHz are compared with the experimental data in Figures 7 and 8. It is seen that the theory agrees quite well with the general trend of the data. The agreement could probably be improved by better choices of the roughness and tilt parameters  $h$  and  $\theta$  and by a more sophisticated treatment of the attenuation of the diffuse component than the simple "average ray" approach.

#### IX. OVERALL LOSS ALONG A PATH WITH ONE CORNER

Table VI gives the overall  $E_h$  mode loss for a path from one tunnel to another, including the corner loss involved in re-establishing the  $E_h$  mode in the second tunnel. The loss is the sum of the corner loss, given in column 3 of Table II and repeated in Table VI, and the straight tunnel loss given in Table V for various total distances. The results in Table VI are for the case of half-wave dipole transmitting and receiving antennas\* and are valid when neither antenna is within about 100 ft. of the corner. The overall loss is smaller than the values in Table VI if the receiving antenna is within this distance, owing to the presence of the rapidly attenuating diffuse component that passes around the corner. From the principle of reciprocity, the same is true if the transmitting antenna is within 100 ft. of the corner.

The results indicate that the optimum frequency lies in the range 400-1,000 MHz. However, if one installs horizontal half-wave resonant scattering dipoles with  $45^\circ$  azimuth in the important tunnel intersections, in order to guide the  $E_h$  mode around the corner, the optimum may shift to somewhat lower frequencies since a greater fraction of the incident  $E_h$  wave will be deflected by the longer low-frequency dipoles.

\* As in the straight tunnel case, refer to Appendix F for the additional loss factors needed to estimate communication range for roving miner applications using portable transceivers.

**FIGURE 7**  
**OVERALL LOSS IN A STRAIGHT TUNNEL IN HIGH COAL**  
**(For Isotropic Antennas)**

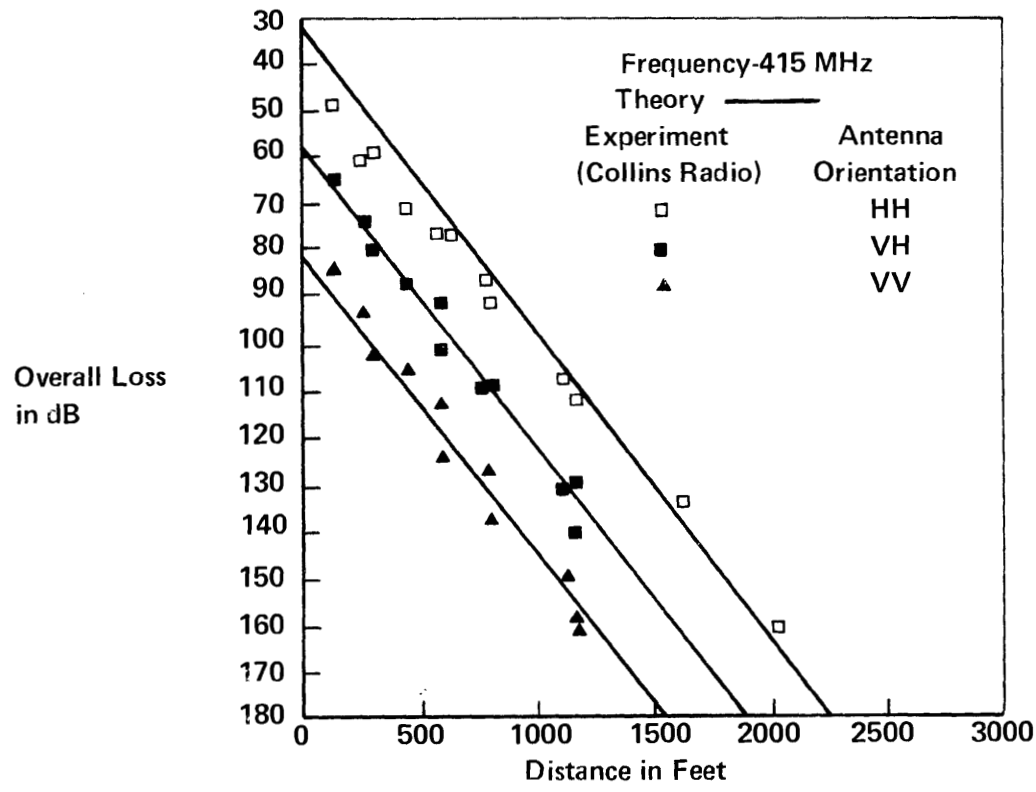
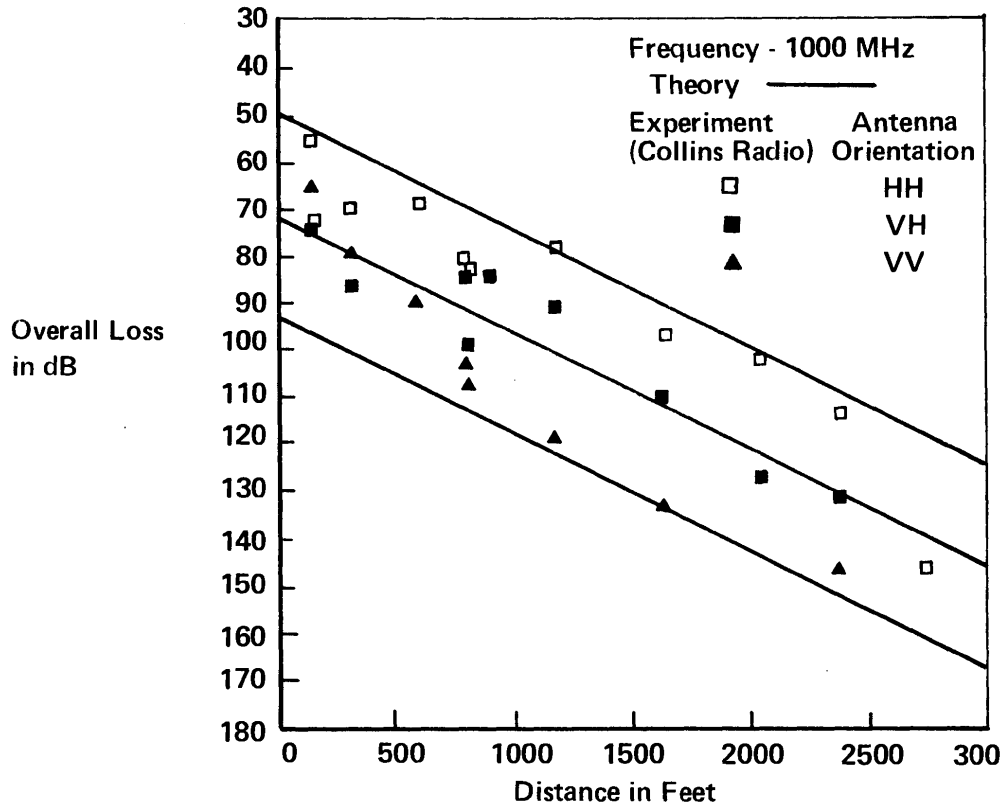


FIGURE 8  
 OVERALL LOSS IN A STRAIGHT TUNNEL IN HIGH COAL  
 (For Isotropic Antennas)



**TABLE VI**  
**OVERALL LOSS ALONG A PATH INCLUDING ONE CORNER**  
 **$E_h$  MODE WITH HALFWAVE DIPOLE ANTENNAS**

f (MHz)	$E_h$ Loss per Corner (dB)	Overall Loss (dB)			
		500'	1000'	1500'	2000'
4000	80.2	177	205	232	259
3000	77.6	163	184	205	226
2000	74.1	147	162	177	192
1000	67.6	126	138	148	161
415	57.7	120	152	184	216
200	47.3	187	308	430	551

## X. CONCLUSIONS

The kind of propagation model developed in this paper, involving the (1,1)  $E_h$  waveguide mode accompanied by a diffuse component in dynamical equilibrium with it, seems to be necessary to account for the many effects observed in the measurement of Collins Radio Company: the exponential decay of the wave; the marked polarization effects in a straight tunnel; the independence of decay rate on antenna orientation; the absence of polarization at the beginning of a cross tunnel; the two-slope decay characteristic in a cross tunnel; and overall frequency dependence. All of these effects are moderately well accounted for by the theoretical model. However, considerable refinement of the theory could be made by removing some of the present oversimplifications, such as: the assumption of perfectly diffuse scattering both in the main tunnel and immediately around a corner in a cross tunnel; the use of the "average ray" approximation; and the description of the propagation around a corner in terms of two asymptotes only.

The last item particularly deserves more attention since we have not included the conversion of the diffuse component in the transition region near the beginning of the cross tunnel into the  $E_h$  mode. For this reason we think that the good fit of the theory to the experimental data in Figures 4 and 5 may be somewhat fortuitous. More data at greater distances down a cross tunnel would be very desirable to settle this question. Data covering a wider frequency range in both main and cross tunnels would also allow a more stringent test of the theory.

## XI. REFERENCES

- (1) E.A.J. Marcatili and R.A. Schmeltzer, "Hollow Metallic and Dielectric Waveguides for Long Distance Optical Transmission and Lasers," The Bell System Technical Journal, Vol 43, 1783, 1964.
- (2) J.I. Glaser, "Attenuation and Guidance of Modes in Hollow Dielectric Waveguides," IEEE Transactions on Microwave Theory and Techniques, March 1969, p. 173; and M.I.T. Ph.D. Thesis, "Low-Loss Waves in Hollow Dielectric Tubes," February 1967.
- (3) Collins Radio Company, Cedar Rapids, Iowa, "Coal Mine Communications Field Test Report," December 29, 1972 prepared for U.S. Department of the Interior, Bureau of Mines, Pittsburgh, Pa.; and a paper entitled "Radio Propagation Measurements in Coal Mines at UHF and VLF," published in Proceedings\*of Through-the-Earth Electromagnetics Workshop at Colorado School of Mines, Golden, Colorado, August 1973.
- (4) P. Beckmann and A. Spizzichino, "The Scattering of Electromagnetic Waves from Rough Surfaces," Macmillan, New York, 1963, p. 81, Eq.(6).
- (5) E.M. Sparrow and R.D. Cess, "Radiation Heat Transfer," Wadsworth Publishing Co., 1966, Appendix A.

---

\* Proceedings to be published as part of Colorado School of Mines Final Report on Bureau of Mines Grant G133023.

APPENDIX A

RAY METHOD

1. Fresnel Formulas

For the Eh mode the reflectances  $R_1$  and  $R_2$  of the vertical and horizontal walls, respectively, are

$$R_1^{Eh} = \left| \frac{K_1 \sin \phi_1 - \sqrt{\sin^2 \phi_1 + K_1 - 1}}{K_1 \sin \phi_1 + \sqrt{\sin^2 \phi_1 + K_1 - 1}} \right|^2 \quad (A1)$$

$$R_2^{Eh} = \left| \frac{\sin \phi_2 - \sqrt{\sin^2 \phi_2 + K_2 - 1}}{\sin \phi_2 + \sqrt{\sin^2 \phi_2 + K_2 - 1}} \right|^2 \quad (A2)$$

For the Ev mode the corresponding formulas are

$$R_1^{Ev} = \left| \frac{\sin \phi_1 - \sqrt{\sin^2 \phi_1 + K_1 - 1}}{\sin \phi_1 + \sqrt{\sin^2 \phi_1 + K_1 - 1}} \right|^2 \quad (A3)$$

$$R_2^{Ev} = \left| \frac{K_2 \sin \phi_2 - \sqrt{\sin^2 \phi_2 + K_2 - 1}}{K_2 \sin \phi_2 + \sqrt{\sin^2 \phi_2 + K_2 - 1}} \right|^2 \quad (A4)$$

2. Loss Rates

Table 1A gives calculated values of grazing angle, number of reflections, reflectance, and loss for the Eh mode in a 14 x 7 high-coal tunnel with  $K_1=K_2=10$ .  $L_1$  and  $L_2$  are the loss rates at the side walls and at the roof and floor, respectively.

TABLE A1

Ray Method Calculations (For Eh Mode)

$f$ (MHz)	$\lambda$ (ft)	$\phi_1$ (deg)	$\phi_2$ (deg)	$N_1$ $\left(\frac{\text{Bounces}}{100 \text{ ft}}\right)$	$N_2$ $\left(\frac{\text{Bounces}}{100 \text{ ft}}\right)$	$R_1$	$R_2$	$L_1$ $\left(\frac{\text{dB}}{100 \text{ ft}}\right)$	$L_2$ $\left(\frac{\text{dB}}{100 \text{ ft}}\right)$	$L$ $\left(\frac{\text{dB}}{100 \text{ ft}}\right)$
1000	0.984	2.0	4.0	0.25	1.00	0.62	0.90	0.51	0.41	0.92
415	2.370	4.9	9.7	0.60	2.42	0.37	0.79	3.05	2.38	5.43
200	4.918	10.1	20.1	1.25	5.02	0.068	0.62	11.40	10.17	21.57

APPENDIX B  
WAVE METHOD

1. (1,1) E<sub>h</sub> and E<sub>v</sub> Modes

The fundamental (1,1) E<sub>h</sub> mode is approximately a TEM wave given by (9) and (10). The complete field of this form in the tunnel ( $-d_1/2 \leq x \leq d_1/2$ ,  $-d_2/2 \leq y \leq d_2/2$ ), satisfying Maxwell's equations, is

$$E_x = E_0 \cos k_1 x \cos k_2 y e^{-ik_3 z} \quad (B1)$$

$$E_y = 0 \quad (B2)$$

$$E_z = \frac{ik_1}{k_3} E_0 \sin k_1 x \cos k_2 y e^{-ik_3 z} \quad (B3)$$

$$H_x = \frac{k_1 k_2}{\omega \mu_0 k_3} E_0 \sin k_1 x \sin k_2 y e^{-ik_3 z} \quad (B4)$$

$$H_y = \frac{(k_1^2 + k_3^2)}{\omega \mu_0 k_3} E_0 \cos k_1 x \cos k_2 y e^{-ik_3 z} \quad (B5)$$

$$H_z = \frac{ik_2}{\omega \mu_0} E_0 \cos k_1 x \sin k_2 y e^{-ik_3 z}, \text{ where} \quad (B6)$$

$$k_1^2 + k_2^2 + k_3^2 = k_0^2 = 4\pi^2/\lambda^2. \quad (B7)$$

Since the wavelengths of interest are small compared with the tunnel dimensions, the wave vector components  $k_1$  and  $k_2$  are small compared with  $k_3$ , which is close to  $k_0 = 2\pi/\lambda$ . Therefore  $H_y$  reduces to the expression given in (10) and  $E_z$ ,  $H_x$ , and  $H_z$  are very small.

In the roof ( $y \geq d_2/2$ ) of dielectric constant  $K_2$ , the field must represent an outgoing wave in the  $y$ -direction and therefore has the form

$$E_x = B \cos k_1 x e^{-ik_2' y} e^{-ik_3 z} \quad (B8)$$

$$E_y = 0 \quad (B9)$$

$$E_z = \frac{ik_1}{k_3} B \sin k_1 x e^{-ik_2' y} e^{-ik_3 z} \quad (B10)$$

$$H_x = \frac{k_1 k_2'}{\omega \mu_0 k_3} B \sin k_1 x e^{-ik_2' y} e^{-ik_3 z} \quad (B11)$$

$$H_y = \frac{(k_3^2 + k_1^2)}{\omega \mu_0 k_3} B \cos k_1 x e^{-ik_2' y} e^{-ik_3 z} \quad (B12)$$

$$H_z = \frac{k_2'}{\omega \mu_0} B \cos k_1 x e^{-ik_2' y} e^{-ik_3 z} \quad (B13)$$

which satisfies Maxwell's equations. The wave number component  $k_2'$  in the dielectric is given by the relation

$$k_1^2 + k_2'^2 + k_3^2 = K_2 k_0^2. \quad (B14)$$

The boundary conditions at  $y = d_2/2$  are that the tangential components of E and H are continuous. These conditions require that

$$E_o = \cos \left( \frac{k_2 d_2}{2} \right) = B e^{-\frac{ik_2' d_2}{2}} \quad (B15)$$

and

$$k_2 E_o \sin \left( \frac{k_2 d_2}{2} \right) = ik_2' B e^{-\frac{ik_2' d_2}{2}}, \quad (B16)$$

from which we obtain the condition

$$k_2 \tan \frac{k_2 d_2}{2} = ik_2' \quad (B17)$$

Since  $k_1$  and  $k_2$  are small compared with  $k_0$  we find from (B7) and (B14) that  $k_2'$  is given approximately by

$$k_2' = k_0 \sqrt{K_2 - 1}. \quad (\text{B18})$$

Therefore, from (B17) and (B18) we obtain the following mode condition for  $k_2$ , for modes that are even functions of  $y$ :

$$k_z \tan \frac{k_2 d_2}{2} = i k_0 \sqrt{K_2 - 1}. \quad (\text{B19})$$

Since  $k_2 d_2 / 2 \ll 1$  we find for the lowest  $E_h$  mode

$$k_2 \approx \frac{\pi}{d_2} - \frac{i\lambda}{d_2^2 \sqrt{K_2 - 1}} \quad (\text{B20})$$

This result shows that, except for a small imaginary part,  $k_2$  has the same value as for a metal waveguide. The imaginary part arises from the power loss due to the outgoing refracted wave.

In the side wall ( $x \geq d_1/2$ ), of dielectric constant  $K_1$ , the field has the form

$$E_x = A e^{-ik_1'x} \cos k_2 y e^{-ik_3 z} \quad (\text{B21})$$

$$E_y = 0 \quad (\text{B22})$$

$$E_z = \frac{k_1'}{k_3} A e^{-ik_1'x} \cos k_2 y e^{-ik_3 z} \quad (\text{B23})$$

$$H_x = \frac{ik_1'k_2}{\omega\mu_0 k_3} A e^{-ik_1'x} \cos k_2 y e^{-ik_3 z} \quad (\text{B24})$$

$$H_y = \frac{(k_1'^2 + k_3^2)}{\omega\mu_0 k_3} A e^{-ik_1'x} \cos k_2 y e^{-ik_3 z} \quad (\text{B25})$$

$$H_z = \frac{ik_2}{\omega\mu_0} A e^{-ik_1'x} \sin k_2 y e^{-ik_3 z} \quad (\text{B26})$$

where

$$k_1'^2 + k_2^2 + k_3^2 = K_1 k_0^2. \quad (\text{B27})$$

Continuity of the tangential E field gives the condition

$$k_1 E_0 \sin\left(\frac{k_1 d_1}{2}\right) = ik_1' A e^{-\frac{ik_1' d_1}{2}} \quad (\text{B28})$$

Continuity of  $H_y$  and  $H_z$  requires that

$$(k_3^2 + k_1^2) E_0 \cos\left(\frac{k_1 d_1}{2}\right) = (k_3^2 + k_1'^2) A e^{-\frac{ik_1' d_1}{2}} \quad (\text{B29})$$

and

$$k_2 E_0 \cos\left(\frac{k_1 d_1}{2}\right) = k_2 A e^{-\frac{ik_1' d_1}{2}} \quad (\text{B30})$$

Since (B29) and (B30) are inconsistent we can only satisfy the H boundary condition approximately. We note that since  $K_1 \gg 1$ ,  $|k_1'|$  is of the same order as  $k_0$ , whereas  $|k_2|$  is much smaller. Therefore we may ignore (B30) and also, from (B7) and (B27), write

$$k_1^2 + k_3^2 \approx k_0^2 \quad (\text{B31})$$

$$k_1'^2 + k_3^2 \approx K_1 k_0^2. \quad (\text{B32})$$

Then from (B28) and (B29) we obtain, approximately,

$$K_1 \tan\left(\frac{k_1 d_1}{2}\right) = \frac{ik_1'}{K_1}. \quad (\text{B33})$$

Again taking advantage of the smallness of  $k_1$  and  $k_2$  relative to  $k_0$ , we find for the lowest  $E_h$  mode that

$$k_1 \approx \frac{\pi}{d_1} - \frac{iK_1 \lambda}{d_1^2 \sqrt{K_1 - 1}}, \quad (\text{B34})$$

which shows that the mode shape in the x-direction is also the same as for a metal waveguide, except for a small imaginary part.

On substituting for  $k_1$  and  $k_2$  from (B33) and (B34) into (B7) we find, on neglecting second order terms, that the propagation constant in the z-direction is

$$k_3 = k_o - \frac{i\lambda^2}{2} \left( \frac{K_1}{d_1^3 \sqrt{K_1-1}} + \frac{1}{d_2^3 \sqrt{K_2-1}} \right) \quad (B35)$$

The power loss in dB for the (1,1)  $E_h$  mode for a distance  $z$  is therefore

$$\begin{aligned} L_{Eh} &= -8.686 \operatorname{Im}(k_3) \\ &= 4.343 \lambda^2 z \left( \frac{K_1}{d_1^3 \sqrt{K_1-1}} + \frac{1}{d_2^3 \sqrt{K_2-1}} \right) \cdot \end{aligned} \quad (B36)$$

We obtain the loss for the (1,1)  $E_v$  mode by interchanging the subscripts 1 and 2 in (B36):

$$L_{Ev} = 4.343 \lambda^2 z \left( \frac{1}{d_1^3 \sqrt{K_1-1}} + \frac{K_2}{d_2^3 \sqrt{K_2-1}} \right) \cdot \quad (B37)$$

As a check on these formulas we find that exactly the same results are obtained if one adds the losses for two infinite slot waveguides of slot widths  $d_1$ ,  $d_2$  and dielectric constants  $K_1$ ,  $K_2$ , respectively. The numerical results given by (B36) and (B37) also agree well with those given by the ray method.

## 2. Higher Modes

One can readily generalize (B36) and (B37) to the case of a higher mode ( $n_1, n_2$ ) with approximately  $n_1$  half-wave loops in the x-direction and  $n_2$  in the y-direction. The results are

$$L_{Eh} (n_1, n_2) = 4.343 \lambda^2 z \left( \frac{n_1^2 K_1}{d_1^3 \sqrt{K_1 - 1}} + \frac{n_2^2}{d_2^3 \sqrt{K_2 - 1}} \right) \quad (B38)$$

$$L_{Ev} (n_1, n_2) = 4.343 \lambda^2 z \left( \frac{n_1^2}{d_1^3 \sqrt{K_1 - 1}} + \frac{n_2^2 K_2}{d_2^3 \sqrt{K_2 - 1}} \right) \quad (B39)$$

Table B1 shows the loss rates for a number of modes for  $f = 1000$  MHz,  $\lambda = 0.98$  ft,  $d_1 = 14$  ft,  $d_2 = 7$  ft,  $K_1 = 10$ ,  $K_2 = 10$ ,  $z = 100$  ft. It is to be noted that formulas (B38) and (B39) become increasingly inexact as  $n_1$  and  $n_2$  increase, since our approximations based on  $k_1, k_2 \ll k_0$  become progressively less valid.

TABLE B1  
LOSS RATES FOR VARIOUS MODES

$n_1$	$n_2$	$L_{Eh}$ (dB/100 ft)	$L_{Ev}$ (dB/100 ft)
1	1	0.9	4.1
1	2	2.1	16.3
2	1	2.4	4.3
2	2	3.6	16.4
1	3	4.2	36.5
3	1	5.0	5.0
2	3	5.7	36.7
3	2	6.2	16.7
3	3	8.2	36.9

## APPENDIX C

### COUPLING OF $E_h$ AND $E_v$ MODES

We first consider the Eh wave incident at a small grazing angle  $\phi_2$  on a perfectly flat and horizontal part of the roof of the tunnel. The reflected wave is then also polarized with the E field horizontal. If the plane on the roof is locally rotated through some angle about the x-direction, i.e., about a transverse horizontal axis, then the E-field in the reflected wave remains horizontal, from symmetry. Rotation about the vertical y-direction also produces no effect since the plane of the roof remains unchanged. Rotation about the z-direction produced by longitudinal ridges can however tilt the E-field of the reflected wave. Figure C1 shows a crosssectional view of the tunnel with the roof rotated through an angle  $\theta$  around the z-axis. The E-field of the incident wave is represented by  $E_i$  and that of the reflected wave by  $E_r$ , which is tilted by an angle  $\delta_2$  relative to  $E_i$ . We wish to calculate  $\delta_2$  in terms of  $\theta$  and the grazing angle of incidence  $\phi_2$ .

Relative to axes  $x'$ ,  $y'$  attached to the rotated portion of the roof the incident E-field has components

$$E_{i,x'} = E_i \cos\theta \quad (C1)$$

$$E_{i,y'} = -E_i \sin\theta. \quad (C2)$$

The reflected field has components

$$E_{r,x'} = E_r \cos(\theta - \delta_2) \quad (C3)$$

$$E_{r,y'} = -E_r \sin(\theta - \delta_2). \quad (C4)$$

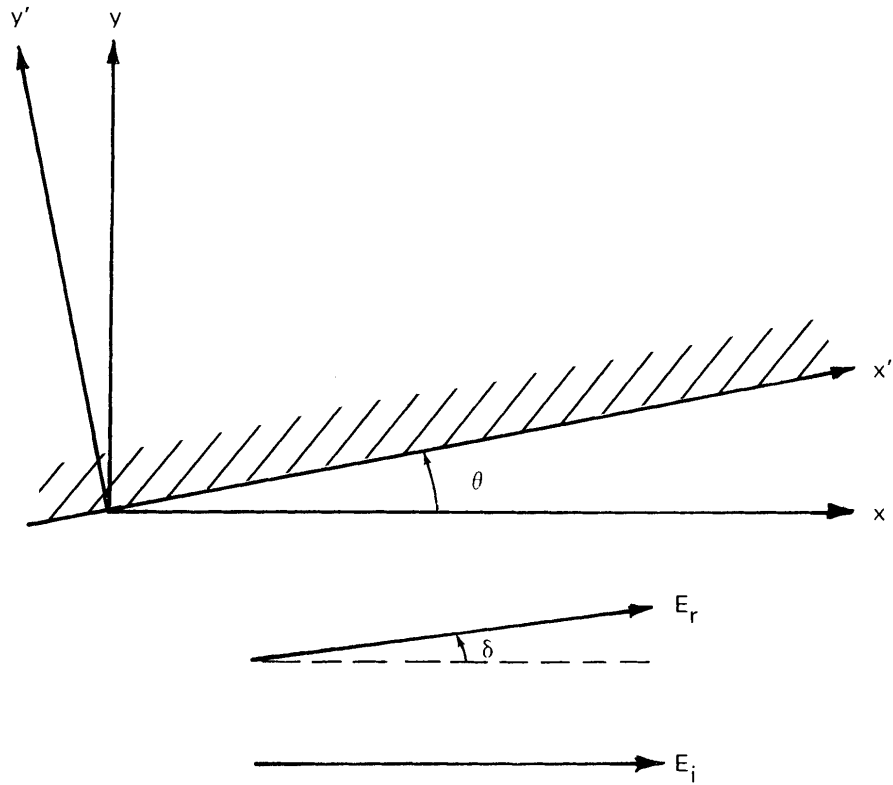


FIGURE C1 INCIDENT AND REFLECTED FIELDS RELATIVE TO A ROTATED PORTION OF THE ROOF OF THE TUNNEL

With respect to the roof the  $x'$  components can be regarded as the TE wave with amplitude reflection  $r_{TE_2}$ . Therefore

$$\frac{E_{r,x'}}{E_{i,x'}} = r_{TE_2}. \quad (C5)$$

Likewise the  $y'$  components act as a TM wave, so that

$$\frac{E_{r,y'}}{E_{i,y'}} = r_{TM_2}. \quad (C6)$$

From (C1)-(C6) we obtain

$$\frac{\tan(\theta - \delta_2)}{\tan\theta} = \frac{r_{TM_2}}{r_{TE_2}}. \quad (C7)$$

This result shows that rotation of the E-field occurs only because  $r_{TM}$  is different from  $r_{TE}$ .

The amplitude reflectances  $r_{TE_2}$  and  $r_{TM_2}$  are given in terms of the grazing angle  $\phi_2$  and the dielectric constant  $K_2$  of the roof by the Fresnel formulas

$$r_{TE_2} = \frac{\sin\phi_2 - \sqrt{\sin^2\phi_2 + K_2 - 1}}{\sin\phi_2 + \sqrt{\sin^2\phi_2 + K_2 - 1}}$$

$$r_{TM_2} = \frac{K_2 \sin\phi_2 - \sqrt{\sin^2\phi_2 + K_2 - 1}}{K_2 \sin\phi_2 + \sqrt{\sin^2\phi_2 + K_2 - 1}} \quad (C9)$$

Equations (C7)-(C9) allow one to calculate the tilt angle  $\delta_2$  of the electric field of the reflected wave for given values of  $\theta$ ,  $\phi_2$  and  $K_2$ . The corresponding equations for the effect of the side walls of the tunnel are

$$\frac{\tan(\theta - \delta_1)}{\tan\theta} = \frac{r_{TE_1}}{r_{TM_1}} \quad (C10)$$

$$r_{TE_1} = \frac{\sin\phi_1 + \sqrt{\sin^2\phi_1 + K_1 - 1}}{\sin\phi_1 - \sqrt{\sin^2\phi_1 + K_1 - 1}} \quad (C11)$$

$$r_{TM_1} = \frac{K_1 \sin\phi_1 - \sqrt{\sin^2\phi_1 + K_1 - 1}}{K_1 \sin\phi_1 + \sqrt{\sin^2\phi_1 + K_1 - 1}} \quad (C12)$$

We have assumed for simplicity that the rms rotation angle  $\theta$  is the same for all four walls of the tunnel. The angles  $\phi_1$  and  $\phi_2$  are given by equations (1) and (2).

We now obtain an expression for the power coupling coefficient between the Eh and Ev modes. From a ray point of view the fraction of the power coupled per reflection is  $\sin^2\delta_1$  for the side walls and  $\sin^2\delta_2$  for the top and bottom walls. The coupling coefficient per foot along the tunnel is therefore

$$\begin{aligned} \alpha_{hv} &= \frac{N_1}{z} \sin^2\delta_1 + \frac{N_2}{z} \sin^2\delta_2 \\ &= \frac{\phi_1}{d_1} \sin^2\delta_1 + \frac{\phi_2}{d_2} \sin^2\delta_2, \end{aligned} \quad (C13)$$

where  $N_1$  and  $N_2$ , the number of reflections for a distance  $z$ , are given by (5) and (6).

It is to be noted that we have added the contributions of the various reflections to  $\alpha_{hv}$  incoherently. The reason is that the Eh and Ev modes are orthogonal, which means that the various contributions from one mode to the other have random phases.

The rate of change of the intensity  $I_v$  in the Ev mode is given by the equation

$$\frac{dI_v}{dz} = -\alpha_v I_v + \alpha_{hv} I_h \quad (C14)$$

where  $I_h$  is the intensity of the Eh mode and  $\alpha_v$  is the attenuation coefficient of the Ev mode due to refraction loss. Now, as will be shown later, the coupling coefficient  $\alpha_{hv}$  is small compared with the loss rates  $\alpha_h$  and  $\alpha_v$  of the two modes. Therefore under steady state conditions both modes decay at a rate close to  $\alpha_h$ . This means that

$$\frac{dI_v}{dz} \approx -\alpha_h I_v. \quad (C15)$$

Thus from (C14) we find that

$$\frac{I_v}{I_h} = \frac{\alpha_{hv}}{\alpha_v - \alpha_h} \quad (C16)$$

Table C1 shows values of  $\delta_1$ ,  $\delta_2$ ,  $\alpha_{hv}$ , and  $I_v/I_h$  calculated by the foregoing equations for three values of the rms rotation angle  $\theta$  of the tunnel walls. The measurements of Collins Radio with the receiving antenna first vertical, then horizontal indicate that  $I_v/I_h$  is in the range -20 to -25 dB for the 1000 and 415 MHz data. Therefore if one assumes that the measured Ev arises entirely from coupling between the two (1,1) modes, a value of  $\theta$  between  $10^\circ$  and  $20^\circ$  is needed to make the theory agree with the experimental data.

TABLE C1

Coupling Between Eh and Ev modes

f (MHz)	$\theta$ (deg)	$\delta_1$ (deg)	$\delta_2$ (deg)	$\alpha_{hv}$ (dB/ft.)	$\alpha_h$ (dB/ft.)	$\alpha_v$ (dB/ft.)	$\frac{I_v}{I_h}$ (dB)
1,000	30	5.5	-6.5	.00066	.010	.0311	-15.0
1,000	20	4.2	-4.7	.00035	.010	.0311	-17.8
1,000	10	2.3	-2.4	.000096	.010	.0311	-23.4
415	30	14.3	-14.4	.0081	.060	.1802	-11.7
415	20	11.6	-10.0	.0042	.060	.1802	-14.6
415	10	6.6	- 5.1	.0012	.060	.1802	-20.0

## APPENDIX D

### PROPAGATION AROUND A CORNER

#### 1. Transmission of Diffuse Component Around a Corner.

To calculate the fraction of the diffuse component in the main tunnel that goes around a corner into a cross tunnel, we use results given in graphical form by Sparrow and Cess<sup>(5)</sup> for the angle factors for diffuse radiation transfer between rectangular areas, on the assumption that the radiation in the main tunnel is perfectly diffuse. In the high coal case of intersecting tunnels each of dimensions 14 ft by 7 ft, the angle factor between the main-tunnel aperture 1 and the cross-tunnel aperture 2 is

$$F_{1 \rightarrow 2} \text{ (High Coal)} = 0.15 = -8.2 \text{ dB} \quad (D1)$$

In the case of low-coal tunnels of dimensions 14 ft x 3.5 ft, the result is

$$F_{1 \rightarrow 2} \text{ (Low Coal)} = 0.10 = -10 \text{ dB} \quad (D2)$$

#### 2. Excitation of Eh Mode in Cross Tunnel by Diffuse Component in Main Tunnel.

Figure D1 depicts the geometry used for computing the degree to which the Eh mode in the main tunnel couples to the Eh mode in a cross tunnel. Diffuse radiation passing through a cross section A of the main tunnel has the angular distribution

$$dP = \frac{P_0 \cos \theta}{\pi A} d\Omega dA \quad (D3)$$

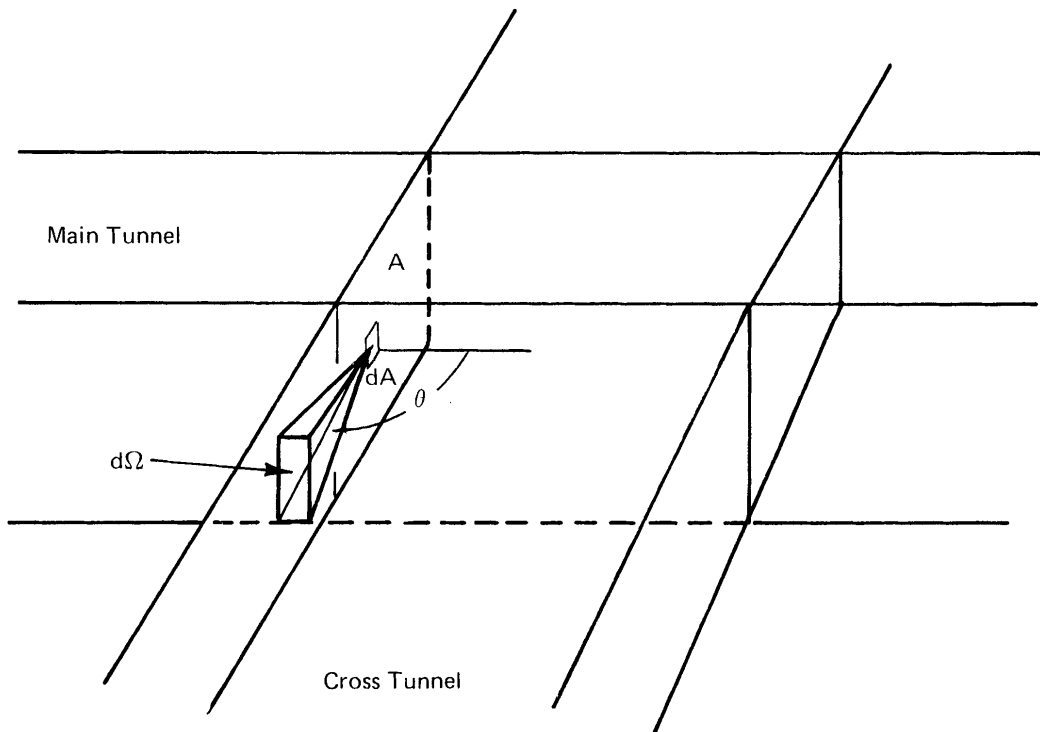


FIGURE D1 GEOMETRY FOR COUPLING TO CROSS TUNNELS

where

$dP$  = power in element of solid angle  $d\Omega$   
from element of area  $dA$

$\theta$  = angle with normal to  $dA$

$P_o$  = total diffuse power

$A$  = total area of cross section

The power entering the Eh mode in the cross tunnel is therefore

$$P = 1/2 \frac{P_o}{\pi A} \int_{\Omega} \int_A \cos\theta d\Omega dA \quad (D4)$$

where the integration is taken over the whole area  $A$  of the cross section and over the solid angle  $\Omega$  of the mode. The factor  $1/2$  allows for the horizontal polarization of the mode.

$$\phi_1 = \lambda/2d_1 \quad (D5)$$

$$\phi_2 = \lambda/2d_2 \quad (D6)$$

$d_1$  and  $d_2$  being the horizontal and vertical dimensions of the tunnel.

Therefore

$$\Omega = 2\phi_1\phi_2 = \frac{\lambda^2}{2d_1d_2} \quad (D7)$$

Since  $\phi_1$  and  $\phi_2$  are small the contributions of various elements  $dA$  are approximately equal since shadowing effects can be neglected. Therefore (D4) becomes

$$\begin{aligned}
 P &= (2\phi_2) \frac{P_o}{2\pi} \int_{\frac{\pi}{2}-\phi_1}^{\pi} \cos\theta \sin\theta d\theta \\
 &= \frac{2\phi_2 P_o}{2\pi} \cdot \frac{1}{2} [1 - \sin^2(\frac{\pi}{2} - \phi_1)] \\
 &= \frac{\phi_2 P_o}{2\pi} (1 - \cos^2\phi_1) \\
 &\approx \frac{\phi_2 \phi_1^2 P_o}{4\pi} \\
 P &= \frac{\lambda P_o}{16\pi d_1^2 d_2} \quad . \quad (D8)
 \end{aligned}$$

The power ratio of the Eh mode in the cross tunnel and main tunnel is

$$\frac{P_{\text{Eh-cross}}}{P_{\text{Eh-main}}} = \frac{P}{P_{\text{Eh-main}}} = \frac{P_o}{P_{\text{Eh-main}}} \cdot \frac{\lambda^3}{16\pi d_1^2 d_2} \quad (D9)$$

where  $P_o$  is the diffuse power level in the main tunnel. This result neglects any contribution from scattering by the floor and roof of the intersection area between the two tunnels.

APPENDIX E

ANTENNA INSERTION LOSS BY CURRENT-DISTRIBUTION METHOD

A half-wave dipole antenna centered at  $x_0, y_0$  in the tunnel and oriented in the x-direction is approximated by a surface current distribution

$$\bar{K}(x,y) = \bar{i}_x I_0 \cos\left(\frac{2\pi x}{\lambda}\right) u_0(y-y_0) \{u_{-1}[x+(x_0 - \frac{\lambda}{2})] - u_{-1}[x-(x_0 + \frac{\lambda}{2})]\} \quad (E1)$$

where  $u_0$  and  $u_{-1}$  are the unit impulse and step functions.

For the case of an infinite tunnel extending to either side of the dipole, the tangential field components take on the usual form

$$\bar{H}_{\pm} = \sum_{j,k} \bar{h}_{jk} \frac{1}{Z_{ojk}} V_{\pm jk} e^{\pm \gamma_{jk} z} \quad (E2)$$

$$\bar{E}_{\pm} = \sum_{j,k} \bar{e}_{jk} V_{\pm jk} e^{\pm \gamma_{jk} z} \quad (E3)$$

$$\bar{h}_{jk} = \bar{h}_{ojk} \cos k_1 x \cos k_2 y \quad (E4)$$

$$\bar{e}_{jk} = \bar{e}_{ojk} \cos k_1 x \cos k_2 y \quad (E5)$$

where  $Z_{ojk}$ ,  $V_{\pm jk}$ ,  $\bar{h}_{ojk}$  and  $\bar{e}_{ojk}$  are the characteristic impedance, + and -wave voltage coefficients, and normalization constants, respectively, for each waveguide mode. By matching the tangential boundary conditions over the cross-section containing the dipole and selecting the dominant (1,1)  $E_h$  mode contribution by using the mode orthogonality properties, we obtain

$$V_{+,1,1} = V_{-,1,1} \quad (E6)$$

$$V_{+,1,1} = -\frac{Z_{o,1,1}}{2} \iint_{x,y} (\bar{i}_z x \bar{K}(x,y)) \cdot \bar{h}_{1,1}(x,y) dx dy \quad (E7)$$

Carrying out the integration we get

$$V_{+,1,1} = \frac{I_o \lambda}{2\pi} Z_{o,1,1} h_{o,1,1} \cos k_1 x_o \cos k_2 y_o \quad (E8)$$

The total power coupled into the dominant (1,1)  $E_h$  waveguide mode propagating in both tunnel directions, to the left and to the right of the dipole, is

$$P_{\text{mode}} = \frac{|V_{+,1,1}|^2}{Z_{o,1,1}} \quad (E9)$$

The power radiated by the dipole is

$$P_{\text{dipole}} = \frac{1}{2} I_o^2 R_r \quad (E10)$$

where  $R_r$  is the dipole radiation resistance. The desired coupling factor  $C$  is the fraction of the dipole radiated power that is coupled to the (1,1)  $E_h$  mode propagating in one of the tunnel directions for a half-wave dipole;  $C$  is given by

$$C = \frac{1/2 P_{\text{mode}}}{P_{\text{dipole}}} = \frac{\lambda^2}{4\pi^2} \frac{Z_{o,1,1}}{R_r} h_{o,1,1}^2 \cos^2 k_1 x_o \cos^2 k_2 y_o. \quad (E11)$$

As in the first method, when the wavelength is small compared with the tunnel cross-sectional dimensions, the cosine factors are approximately zero at the tunnel walls, so that  $k_1 \cong \pi/d_1$ ,  $k_2 \cong \pi/d_2$  and  $h_{o,1,1} \cong \frac{2}{\sqrt{d_1 d_2}}$ . In addition  $Z_{o,1,1}$  and  $R_r$  become, to good approximation, 377 ohms and 73 ohms, respectively, their corresponding free space values. Under these conditions (E11) becomes

$$C = 0.52 \frac{\lambda^2}{d_1 d_2} \cos^2 \frac{\pi x_o}{d_1} \cos^2 \frac{\pi y_o}{d_2}. \quad (E12)$$

## APPENDIX F

### EXPECTED COMMUNICATION RANGE BETWEEN TWO ROVING MINERS

Communication can be maintained between two separated individuals until the separation distance increases to a point where the signal strength is not sufficient to overcome the background electrical noise. To obtain estimates of this communication range for a mobile application involving roving miners equipped with portable handy talkie transceivers, three frequency independent loss factors should be added to the values of overall loss presented in Tables V and VI. These factors are: -polarization loss-to account for likely misalignment of transmit and receive antennas, -antenna efficiency loss-to account for the non-ideal antenna installation on handy talkies, and -fade margin-to account for signal cancellation effects due to destructive interference. Nominal values which appear reasonable for these factors are 12dB, 4dB, and 12dB, respectively, resulting in a total of 28dB to be added to the above mentioned values of overall loss. By exercising care in the orientation and position of the handy talkies in the mine tunnel cross-section while communicating, these polarization and signal fading losses can of course be reduced, thereby producing a corresponding increase in range.

Representative values of receiver sensitivity and transmitter power for FM portable handy talkies in the UHF 450-MHz band are 0.5 microvolt for 20dB of quieting (-113 dBm into a 50-ohm input resistance) and 2 watts (33 dBm), respectively, resulting in a total allowable loss of 146dB. In this frequency band measurements in mines have shown that the intrinsic electrical noise of the UHF receiver will predominate over externally generated electrical noise. Using the above parameter values in conjunction with the 415-MHz overall loss values presented in Tables V and VI for straight line transmission paths and paths including one corner, predictions of communication range along haulageways and in working sections of mines can be obtained, as shown in Figure F1. Figure F1 illustrates the coverage expected in a high-coal mine between a centrally located miner with a handy talkie unit and a second miner roving throughout a typical 600 x 600 foot mine section with another unit at an operating frequency of 415 MHz.

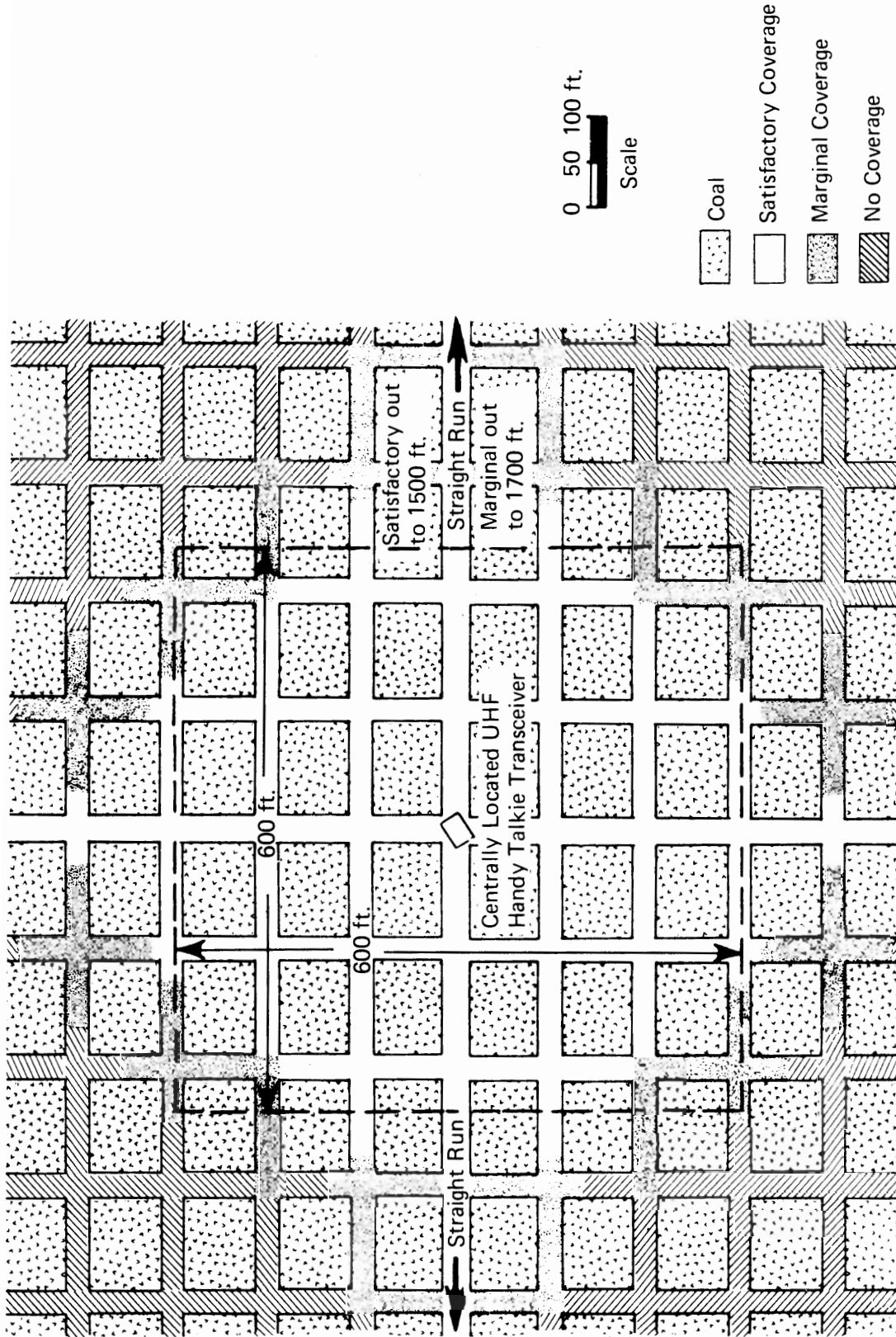


FIGURE F1 PREDICTED UHF WIRELESS RADIO COVERAGE  
For 2-Watt Handy Talkies in a High (7-foot) Coal Mine Section  
Frequency — 415 MHz

When the signal must go around only one corner, satisfactory communication can be expected over a linear distance of approximately 500 feet down an entry and cross-cut. When no corners are encountered, as in a haulageway transmission path, satisfactory straight line communication can be expected over distances in excess of 1500 feet. These range limits are somewhat conservative estimates, and as mentioned above, can usually be somewhat extended if the handy talkies are rotated into the horizontal plane, pointed across the tunnel, and translated a little to a more favorable signal strength position, thereby taking full advantage of the dominant horizontal field component and minimizing destructive interference effects.

Wireless coverage was estimated using the 415 MHz frequency results because the 450 MHz UHF frequency band is the present upper limit for commercially available portable radio transceivers, and because operating frequencies near 400 MHz are most favorable for high-coal section applications where transmission paths typically include one corner. Additional information regarding the practical application of UHF wireless radio systems to mine haulageways and sections is given in a paper coauthored by R. Lagace of ADL and H. Parkinson of PMSRC entitled "Two-Way Communications with Roving Miners," and published in U.S. Bureau of Mines Information Circular No. 8635.